Short Communication

Earthquake-induced clastic dyke and fluid inflow at the Miguel Burnier manganese-ore deposit, Quadrilátero Ferrífero of Minas Gerais, Brazil

Tiago Henrique DeFerreira[1,2] · Alexandre Raphael Cabral[1,3] · Francisco Javier Rios[1]

Received: 3 November 2020 / Accepted: 28 January 2021 / Published online: 17 February 2021

Abstract
A clastic dyke has been recognised within manganese (Mn)-rich Cenozoic sediments near a historical Mn-ore deposit in the Miguel Burnier district, Quadrilátero Ferrífero, in the southern São Francisco craton, Brazil. Here, we describe the clastic dyke, a subvertical fissure that is filled with friable arenaceous fragments, and characterise it as seismite. An overprint by stockwork-like Mn-oxide veinlets and Mn-oxide dissemination, mineralogically expressed as birnessite, lithiophorite and jianshuiite, and geochemically represented by metalliferous enrichments, particularly mercury (Hg), occurs in the clastic dyke and its immediate vicinity. Such an overprint also contains illite, which forms a mineral association with birnessite, lithiophorite and jianshuiite, and constrains the temperature of hydrothermal alteration to less than 300 °C. The recognition of seismite and its Hg enrichment indicate that the Cenozoic history of the Quadrilátero Ferrífero cratonic terrane has been affected by seismic episodes, which were not only conducive to local enrichment in Mn at Miguel Burnier, but also to the dam failure of the 5th of November 2015 (Agurto-Detzel et al. in Geophysical Research Letters 43: 4929–4936, 2016).

Keywords Seismite · Clastic dyke · Cenozoic tectonics · São Francisco craton · Quadrilátero Ferrífero · Metal enrichment

1 Introduction

Earthquakes are not only marked by sudden brittle failure of rock masses that occasionally causes devasting effects on human communities, but also by certain features that can be preserved in the geological record. As brittle fracturing is a recurrent process associated with cracking and sealing that involves fault-channelled fluid inflow, its preservation in the geological record can be manifested in the form of metalliferous concentrations of economic significance [1–3]. In addition, recognising earthquake-related features, deformation structures of seismic origin in rocks and soft sediments, is the fundamental course of action in palaeoseismological analysis [4, 5].

Deformation structures that are genetically related to earthquakes, notwithstanding the caveats highlighted by Shanmugam [6], are known as seismites, a term that was originally proposed by Seilacher [7, 8]. The identification of seismites is challenging. Where firmly recognised, however, a seismite does mainly indicate the seismotectonic character of a region [9–12]. Particularly challenging is the identification of seismite in tropical regions, where deep weathering obscures geological structures [13]. This is the case of lateritic covers on tectonically stable cratonic terranes.

Supplementary information The online version contains supplementary material available at (https://doi.org/10.1007/s42452-021-04297-x).

✉ Tiago Henrique DeFerreira, tiagohdeferreira@gmail.com | [1]Centro de Desenvolvimento da Tecnologia Nuclear (CNEN), Av. Presidente Antônio Carlos, 6627, Campus UFMG Pampulha, Belo Horizonte, MG 31270-901, Brazil. [2]Graduate Programme of Centro de Desenvolvimento da Tecnologia Nuclear (CDTN/CNEN), Belo Horizonte, Brazil. [3]Centro de Pesquisas Professor Manoel Teixeira da Costa (CPMTC), Instituto de Geociências, UFMG, Belo Horizonte, MG, Brazil.

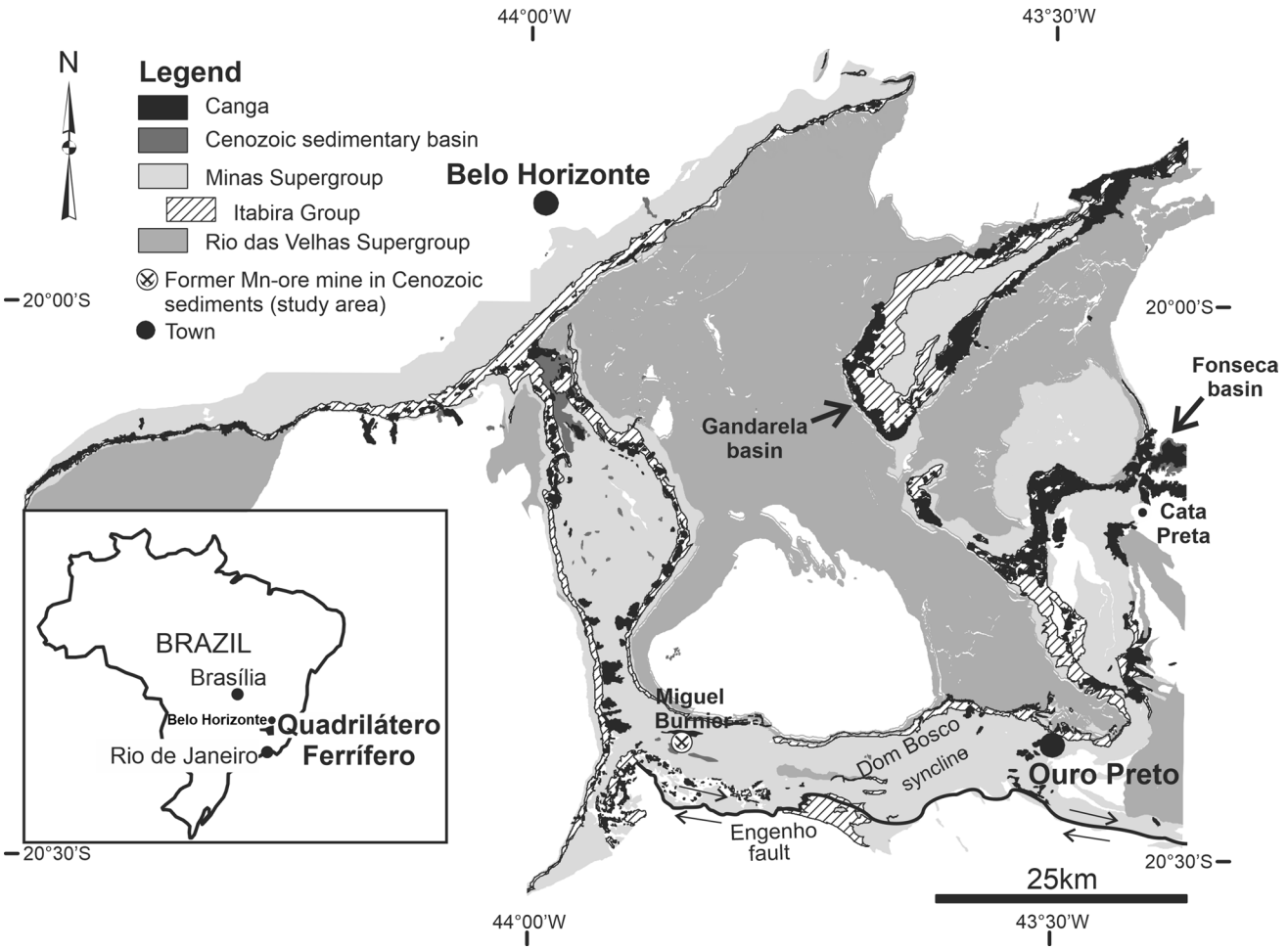

Fig. 1 Simplified geological map of the Quadrilátero Ferrífero [35, 79], with emphasis on the distribution of canga plateaux and Cenozoic basins. The study area, Miguel Burnier, is located in the western extreme of the Dom Bosco syncline, the southern border of which is marked by the Engenho strike-slip fault

The cratonic terrane of the Quadrilátero Ferrífero, located in the southernmost part of the São Francisco craton [14], is one of the most geologically investigated regions in the world (Fig. 1). While much attention has been dedicated to the Precambrian tectonics of the Quadrilátero Ferrífero [15–22], only a few authors have carried out tectonic studies involving small Cenozoic basins, a few km across, which are sparsely distributed in the Quadrilátero Ferrífero [23–28]. The opening of such sedimentary basins over the Precambrian terrane of the Quadrilátero Ferrífero indicates that the region was tectonically, and perhaps seismically, active in the Cenozoic. Evidence for hodiern seismic activity comes from small-magnitude earthquakes that have been registered in the Quadrilátero Ferrífero. Agurto-Detzel et al. [29] related the dam failure of mine tailings and subsequent flood in Mariana, 80 km ENE of our study area at Miguel Burnier, on the 5th of November 2015, to several earthquakes of small magnitude, from 1.3 to 2.6. A 3.5-magnitude earthquake took place on the 25th of November 2019, the epicentre of which was 25 km W of Miguel Burnier [30].

Here, we report the finding of a clastic dyke that is incised into unmetamorphosed sediments of a Cenozoic basin in the Quadrilátero Ferrífero. The clastic dyke is located near a historical Mn-ore deposit in the Miguel Burnier district of Ouro Preto, the first and largest Mn-ore mining site in Brazil in the period from the late-nineteenth to the early-twentieth century [31–33]. We characterise the clastic dyke as seismite, its associated metalliferous enrichment, and discuss its implications.

2 Geological setting

The structural framework of the Quadrilátero Ferrífero resulted from two main deformational events, the Transamazonian and the Brasiliano [17, 34]. The former was an extensional event of Palaeoproterozoic age, between 2.1

and 1.7 Ga, which is thought to have led to the emplacement of Archaean granite–gneiss domes and the nucleation of regional synclines and fault systems, comprising supracrustal rocks of the Rio das Velhas Supergroup and the Minas Supergroup [35]. Relevant to this study are the Dom Bosco syncline and the Engenho strike-slip fault [31, 36]. The second event was compressive and marked the closure of the Pan-African/Brasiliano proto-ocean (0.65–0.50 Ga). The Brasiliano event is mainly recorded in the eastern border of the Quadrilátero Ferrífero as a west-verging, fold-and-thrust belt [17, 34]. The aforementioned structural development is, nevertheless, not consensual. For different views, see for instance Hippertt and Davis [37] and Endo et al. [38].

Cenozoic basins are sparsely distributed in the Quadrilátero Ferrífero [35, 39, 40]. They are small graben-like basins, reaching a few km across, in which sediments accumulated over Precambrian rocks, from the Late Eocene to the Early Miocene [40, 41]. Many Cenozoic basins are located in Precambrian rocks of the Itabira Group of the Minas Supergroup [35], previously known as the Itabira iron formation [42]. The Itabira Group consists of itabirite—i.e., a metamorphosed, banded Fe-oxide-rich rock, which grades upwards to dolomitic rocks.

One of such Cenozoic basins is the Fonseca basin, located in the eastern border of the Quadrilátero Ferrífero (Fig. 1). There, normal faults were observed in Oligocene–Miocene sediments [28, 43]. Importantly, clastic dykes were recorded in Quaternary sediments covering the Fonseca basin—i.e., a plateau of conglomeratic deposits of itabirite-derived ironstone pebbles, cemented by Fe oxyhydroxide [28].

3 Methods

Samples collected during fieldwork were dried in a furnace at 60 °C, crushed and ground in an agate mill. Their powders were then investigated by X-ray diffraction (XRD), using a RIGAKU X-ray diffractometer, model D\MAX ULTIMA IV, housed at CDTN (Centro de Desenvolvimento da Tecnologia Nuclear). The instrument operated from 4° to 80° (2θ angle) at 40 kV and 30 mA, and goniometer speed of 4°2θ/min. Mineral identification was carried out following the database of the International Centre for Diffraction Data and the Joint Committee on Powder Diffraction Standards—JCPDS. Diffractograms and XRD tables are presented in the Electronic Supplementary Material.

Samples were also measured for As, Ag, Cd, Sb, Te, Hg, Pt, Au, Pb and Pd at Bureau Veritas Commodities Canada Ltd., Vancouver, by inductively coupled plasma–mass spectrometry (ICP–MS), following aqua regia digestion.

4 Study area and results

A dyke-like structure occurs 1 km W of the historical Mn-ore mining area in the Miguel Burnier district (Fig. 1; UTM coordinates: 23K 628307; 7739935). The historical mining focussed on Mn ore that was believed to be a residual deposit, derived from the weathering of Precambrian dolomite and manganiferous itabirite (Fig. 2) [33]. However, our field observations in the remains of the historical mining area have indicated that the Mn ore was hosted in Cenozoic sediments. The dyke-like structure is subvertical, incised into Mn-rich mudstone of a Cenozoic basin (Fig. 3a). The 1.3-m-wide dyke is made up of pebble-to-boulder-sized fragments of friable sandstone, which consists essentially of medium-to-coarse-grained quartz sand, with some illite, rutile and hematite. The dyke walls are approximately planar, trending 080° and slightly funnelling downward. Its exposure is roughly cuneiform within a collapsed Mn-rich mudstone wall rock (Fig. 3b).

The clastic dyke truncates Mn-rich mudstone underneath a lateritic cover of canga—i.e., a ferruginous duricrust. The Mn-rich mudstone is a fine-grained rock consisting of clay- and silt-sized particles of hydrous Mn oxide, hematite, kaolinite and quartz. Sandstone lenses occur within the Mn-rich mudstone. An interlocking network of Mn-oxide veinlets, resembling stockwork, occurs in the clastic dyke and its immediate vicinity. Stockwork-like Mn-oxide veinlets are spatially associated with brecciated arenaceous fragments within the dyke (Fig. 3c). The Mn-oxide veinlets are made up of birnessite, lithiophorite, illite and jianshuiite, and minor quartz and hematite. The central part of the clastic dyke has an approximately 20-cm-thick Mn-oxide zone, in which fine-grained Mn oxide is

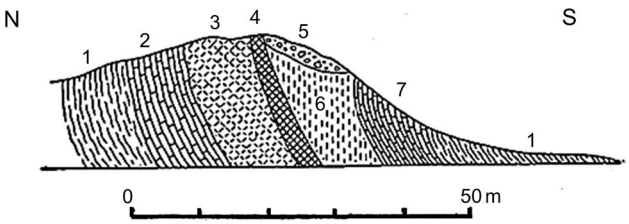

Fig. 2 Geological cross section of the Miguel Burnier mine according to Scott [33]. Manganese-ore mining targeted on a layer of variable thickness, the average of which was 3 m. It was mainly composed of hard metallic and soft, hydrated Mn ore (4). The metallic ore made up, on average, 80% of the layer. It occurred as lenses or irregular bodies. The ore seam was underlain by earthy and impure Fe ore and Mn ore, up to 24 m in thickness (3), and overlain by a body of friable hematite, known as jacutinga, and itabirite (6). Above the itabirite there was grey limestone (7), and below the earthy material, white limestone (2). Iron-ore conglomerate and duricrust (5) partially covered the previously described rocks, excepting the ferruginous schist (1)

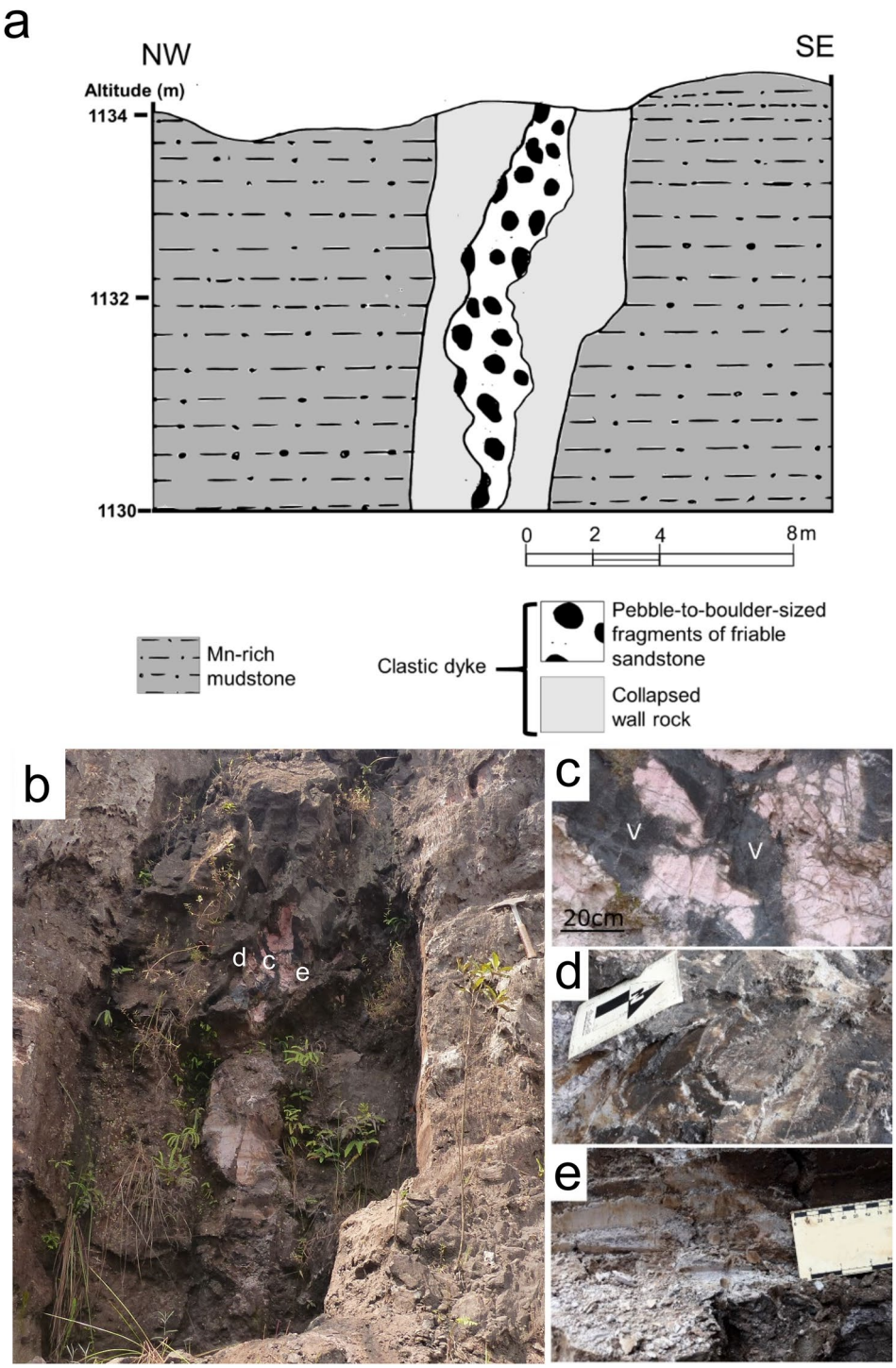

Fig. 3 **a** Schematic geological cross section of the clastic dyke, emphasising its diagnostic attributes. **b** Photograph, looking 176°, of a subvertical fissure that is filled with fragments of friable sandstone, incised into Mn-rich mudstone. **c** Zoomed-in photograph towards 030° of the site indicated in *b*, showing a fragment of friable sandstone that is cross-cut by Mn-oxide veins (v). The latter cement sandstone fragments within the clastic dyke. Stockwork-like Mn-oxide veinlets occur in the immediate vicinity of a brecciated sandstone fragment (*upper right*). **d** Photographic detail, looking 113°, of the site marked in *b*, displaying an approximately 20-cm-thick zone of Mn-oxide dissemination as a dark-brown matrix, with whitish veinlets of illite and quartz. **e** Photographic close-up towards 176° of the site labelled in *b* to illustrate a whitish zone rich in illite

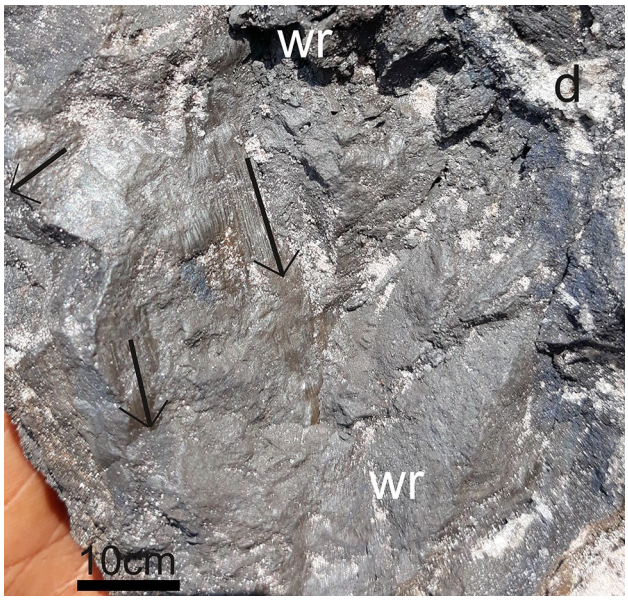

Fig. 4 Photograph of an oriented sample taken from the contact between the dyke and its wall rock. Arrows indicate slickenside lineation at the contact with the clastic dyke. The lineation plunge varies from 120°/33° to 065°/30° on the slickenside, the orientation of which is 127°/30°. Labels wr and d stand for wall rock and clastic dyke, respectively

disseminated, yielding a dark-brown matrix with whitish veinlets (Fig. 3d). The matrix of the Mn-oxide dissemination has birnessite, jianshuiite, quartz, rutile and minor hematite, whereas the whitish veinlets comprise illite and quartz. Besides the Mn-oxide dissemination, the dyke infill displays a 20-cm-thick zone of whitish-grey shades (Fig. 3e). This whitish-grey zone has illite and quartz as the main constituents, and minor amounts of lithiophorite and birnessite. Slickenside striae on the SE-dipping wall of the dyke are oriented at 120°/33° and 065°/30° (Fig. 4).

Table 1 displays the results of reconnaissance whole-rock chemical analyses for Sb, Hg, As, Cd, Te, Pb and precious metals within the clastic dyke and its vicinity. Compared to the upper continental crust (UCC, [44, 45]), the clastic dyke and its stockwork-like Mn-oxide veinlets and Mn-oxide dissemination have enrichments in Au, Hg, Te and Sb, which reach between 10 and 100 times, whereas Cd attains its maximum between 100 and 1000 times (Fig. 5).

5 Discussion

The dyke-like structure found at Miguel Burnier resembles that of a clastic dyke, which represents infilling of open fissures, either by gravity or tectonic stretching. Clastic dykes, also known as sedimentary dykes, are categorised as: (a) neptunian dykes, which are fissures that are filled with superficial material [46], and (b) intrusion dykes, the infilling material of which comes from below. Both categories are seismically induced [47–49]. Clastic dykes have thus been characterised as seismites [49].

It is difficult to reconcile the straight contacts and the cuneiform cross section of the Miguel Burnier clastic dyke with a non-seismic slope process, such as creep. Field evidence suggests that sandstone fragments and arenaceous material collapsed from the surface into a vertical fissure that was tectonically opened, as indicated by slickenside grooves (Fig. 4). The latter are indicators of seismic slip [50]. Furthermore, the groove lineation of Fig. 4 plunges from 120°/33° to 065°/30°, pointing to an oblique strike-slip component of movement. Such a strike-slip component can tentatively be understood as reactivation of the Engenho strike-slip fault in the vicinity of Miguel Burnier (Fig. 1) [31, 51], in a way similar to the reactivation of the Água Quente fault system, as suggested by the

Table 1 Chemical analyses for Sb, Hg, As, Cd, Te, Pb and precious metals in the clastic dyke and its immediate vicinity

		Minimum limit of detection	Stockwork-like Mn-oxide veinlets	Brecciated arenaceous fragments within the dyke	Mn-oxide dissemination	Whitish-grey zone
As	ppm	0.1	9.5	0.3	44.4	1.8
Pd	ppb	10	31	< 10	< 10	< 10
Ag	ppb	2	141	14	152	11
Cd	ppm	0.01	35.45	0.01	0.11	1.98
Sb	ppm	0.02	0.40	0.07	39.89	0.78
Te	ppm	0.02	0.38	0.13	0.31	0.19
Pt	ppb	2	7	17	4	4
Au	ppb	0.2	4.3	7.0	74.9	0.4
Hg	ppb	5	1086	14	1778	83
Pb	ppm	0.01	18.11	4.10	41.55	13.72

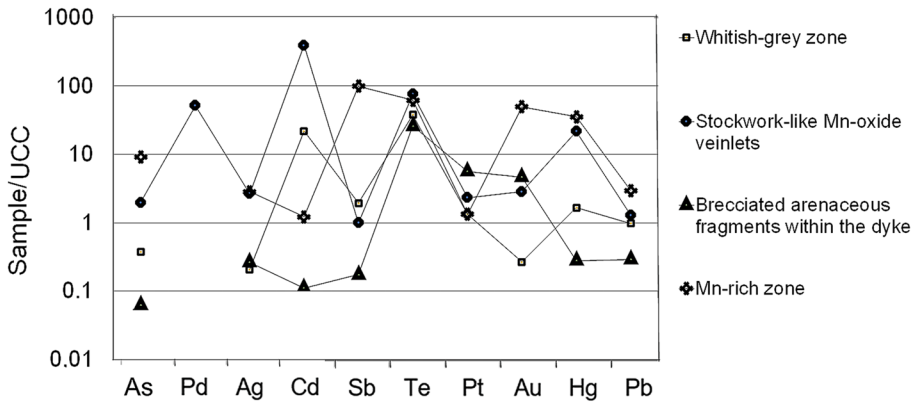

Fig. 5 Plot of precious metals, Sb, As, Hg, Cd, Te and Pb, normalised to the upper continental crust (UCC), in rock samples from the clastic dyke and its immediate vicinity, Miguel Burnier. It is notable that Hg and Te reach 1778 ppb and 0.38 ppm, respectively, within the zone of stockwork-like Mn-oxide veinlets and Mn-oxide dissemination. Cadmium has up to 35 ppm in the stockwork-like Mn-oxide veinlets. Antimony attains 40 ppm in the zone of Mn-oxide dissemination. All UCC values, excepting Te, are from Hu and Gao [44]; average UCC value for Te comes from Wedepohl [45]

deformational and hydrothermal overprint on Cenozoic sediments in the eastern Quadrilátero Ferrífero [28, 52].

Another line of evidence that favours a seismogenic nature for the clastic dyke is the overprint of the dyke infill by stockwork-like Mn-oxide veinlets and Mn-oxide dissemination [53–55]. Manganese-oxide minerals, such as birnessite, lithiophorite and jianshuiite, are known from low-temperature hydrothermal systems [56–61]. The dyke infill and wall-rock overprint also contain illite, which is a low-temperature hydrothermal mineral formed below 300 °C [62–64]. Interestingly, illitisation as a low-temperature hydrothermal overprint is recorded from Cenozoic sediments in the eastern part of the Quadrilátero Ferrífero at Cata Preta (Fig. 1) [52].

Additionally, reconnaissance whole-rock chemical analyses identified a remarkable enrichment in Hg. According to Yangfen et al. [65] and Zhang et al. [66], Hg becomes so distinctly elevated in groundwater during earthquakes that Hg can be used as an indicator of seismic activity. Furthermore, Hg and Sb are known to be typically enriched in hot-spring deposits. Their enrichment in the Mn-oxide veinlets is comparable to those found in modern hot springs [56, 67–69]. Such enrichments suggest that the clastic dyke was formed due to seismic rupturing followed by fluid inflow, hydrothermally overprinting the Cenozoic sediments within the dyke and its surroundings.

The recognition of hydrothermal overprint on Cenozoic sediments following seismic rupturing might provide an alternative interpretation to some mineral occurrences in the Quadrilátero Ferrífero, such as the cinnabar of Tripuí, Ouro Preto, 30 km E of the clastic dyke described here. There, cinnabar was observed in gravels cemented by limonite and pyrolusite [70]. Elsewhere in the Quadrilátero Ferrífero, considerable amounts of Hg have been recognised in Mn-oxide-rich rocks in weathered profiles with fault-related fabrics [53, 54], and also in brittle fractures that are healed by Mn oxides containing Hg [71]. Both occurrences can be explained by deformational and hydrothermal activity during the Cenozoic.

The mudstone wall rock of the clastic dyke is analogous to that attributed to Cenozoic sediments elsewhere in the Quadrilátero Ferrífero [31, 40, 43, 72]. Palynological studies of other Cenozoic sedimentary basins, such as the Fonseca and Gandarela basins (Fig. 1) [40, 41], suggest that the sedimentation at Miguel Burnier is no older than the Late Eocene. It can thus be inferred that the clastic dyke is no older than ca. 38 Ma. Radiogenic dating of goethite that cements the lateritic cover of canga indicates (U–Th)/He ages from 48 to < 2 Ma [73]. It means that the seismically induced fissure responsible for the clastic dyke was coeval with the prolonged history of deep lateritic weathering in the Quadrilátero Ferrífero [73, 74].

Deep lateritic weathering in the Quadrilátero Ferrífero is topographically expressed as canga plateaux. It is pertinent to point out that much of the topography of the Quadrilátero Ferrífero region, in particular its canga plateaux, has been attributed to extensional tectonics [28, 75]. The regional topography of the Quadrilátero Ferrífero and its drainage systems are thought to have resulted from tectonically uplifted and depressed blocks [28, 76]. Such lines of evidence further support the characterisation of the clastic dyke as seismite. Present-day seismicity has been recorded in the Quadrilátero Ferrífero and its surroundings [29, 77, 78].

Combined with hodiernal seismicity, which was conducive to the catastrophic dam failure on the 5th of November 2015 [29], the earthquake-induced dyke indicates that the Quadrilátero Ferrífero has seismically been active since the Late Eocene. It further indicates that hydrothermal

overprint of low temperature yielded local concentration of Mn at Miguel Burnier. Local concentration of Mn and other metals, notably Hg, has recently been documented elsewhere in the Quadrilátero Ferrífero and related to seismic rupturing and fluid inflow [53, 54].

6 Conclusion

A subvertical fissure that is filled with sandstone fragments occurs at Miguel Burnier, a historical site of Mn-ore mining in the Quadrilátero Ferrífero. The fissure is a clastic dyke, formed in response to seismic rupturing. The clastic dyke and its vicinity have metalliferous enrichments (Mn, Hg, Sb, Cd and Te). Earthquake-induced fluid inflow could have played some role in the Mn mineralisation of Miguel Burnier and elsewhere in the Quadrilátero Ferrífero. Our observations indicate that the southernmost São Francisco craton has seismically been active since the Late Eocene.

Acknowledgements We acknowledge CNPq [Grant number 424909/2016-2], FAPEMIG [Grant number PPM-00357-17], FINEP, CDTN/CNEN and CAPES for grants, and a M.Sc. scholarship to the first author. We are grateful to Professor Bernd Lehmann for financing the costs of reconnaissance whole-rock chemical analyses. We are indebted to the anonymous reviewers for their thoughtful comments that substantially improved the original manuscript. We are also grateful to Dr. Clifford Chuwah for his editorial handling and comments.

Funding Our project was funded by CNPq [Grant number 424909/2016–2], FAPEMIG [Grant number PPM-00357–17], FINEP, CDTN / CNEN and CAPES.

Compliance with ethical standards

Conflict of interest On behalf of all authors, the corresponding author states that there is no conflict of interest.

References

1. Sibson RH (1987) Earthquake rupturing as a mineralizing agent in hydrothermal systems. Geology 15(8):701–701. https://doi.org/10.1144/gsjgs.131.6.0653
2. Sibson RH (1992). Earthquake faulting, induced fluid flow, and fault-hosted gold-quartz mineralization. In: Mogk D, Mason R (Eds.), *Basement Tectonics 8. Proceedings of the International Conferences on Basement Tectonics*, vol 2. (pp. 603–614). Dordrecht: Springer
3. Weatherley DK, Henley RW (2013) Flash vaporization during earthquakes evidenced by gold deposits. Nat Geosci 6:294–298. https://doi.org/10.1038/ngeo1759
4. Fuller ML (1912) The New Madrid earthquake. USGS Bulletin 494. https://doi.org/10.3133/b494
5. Vittori E, Sylos Labini S, Serva L (1991) Palaeoseismology: review of the state-of-the-art. Tectonophysics 193(1–3):9–32. https://doi.org/10.1016/0040-1951(91)90185-U
6. Shanmugam G (2017) The fallacy of interpreting SSDS with different types of breccias as seismites amid the multifarious origins of earthquakes: implications. J Palaeogeogr 5(4):318–362. https://doi.org/10.1016/j.jop.2016.09.001
7. Seilacher A (1969) Fault-graded beds interpreted as seismites. Sedimentology 13(1–2):155–159. https://doi.org/10.1111/j.1365-3091.1969.tb01125.x
8. Seilacher A (1984) Sedimentary structures tentatively attributed to seismic events. Mar Geol 55(1–2):1–12. https://doi.org/10.1016/0025-3227(84)90129-4
9. El Taki H, Pratt BR (2012) Syndepositional tectonic activity in an epicontinental basin revealed by deformation of subaqueous carbonate laminites and evaporites: Seismites in Red River strata (Upper Ordovician) of southern Saskatchewan. Can Bull Can Pet Geol 60(1):37–58. https://doi.org/10.2113/gscpgbull.60.1.37
10. Moretti M (2000) Soft-sediment deformation structures interpreted as seismites in Middle–Late Pleistocene Aeolian deposits (Apulian foreland, southern Italy). Sed Geol 135:167–179. https://doi.org/10.1016/S0037-0738(00)00070-1
11. Moretti M, Sabato L (2007) Recognition of trigger mechanisms for soft-sediment deformation in the Pleistocene lacustrine deposits of the Sant'Arcangelo Basin (Southern Italy): Seismic shock vs. overloading. Sediment Geol 196(1–4):31–45. https://doi.org/10.1016/j.sedgeo.2006.05.012
12. Novak A, Egenhoff S (2019) Soft-sediment deformation structures as a tool to recognize synsedimentary tectonic activity in the middle member of the Bakken Formation, Williston Basin, North Dakota. Mar Pet Geol 327:296–313. https://doi.org/10.1016/j.marpetgeo.2019.04.012
13. Rossetti DF, Alves FC, Valeriano MM (2017) A tectonically-triggered late Holocene seismite in the southern Amazonian lowlands, Brazil. Sediment Geol 358:70–83. https://doi.org/10.1016/j.sedgeo.2017.07.003
14. Almeida FFM (1977) O Cráton do São Francisco. Braz J Geol 7:349–364. https://doi.org/10.5327/rbg.v7i4.128
15. Alkmim FF, Martins-Neto MA (2012) Proterozoic first-order sedimentary sequences of the São Francisco craton, eastern Brazil. Mar Pet Geol 33(1):127–139. https://doi.org/10.1016/j.marpetgeo.2011.08.011
16. Carneiro MA, Teixeira W, Carvalho Junior IMD, Fernandes RA (1998) Ensialic tectonic setting of the Archaean Rio das Velhas greenstone belt: Nd and Pb isotopic evidence from the Bonfim metamorphic complex, Quadrilátero Ferrífero. Brazil Revista Brasileira de Geociências 28(2):189–200. https://doi.org/10.25249/0375-7536.1998189200
17. Chemale F, Rosière CA, Endo I (1994) The tectonic evolution of the Quadrilátero Ferrífero, Minas Gerais, Brazil. Precambr Res 65(1–4):25–54. https://doi.org/10.1016/0301-9268(94)90098-1
18. Cutts K, Lana C, Alkmim F, Farina F, Moreira H, Coelho V (2019) Metamorphism and exhumation of basement gneiss domes in the Quadrilátero Ferrífero: two stage dome-and-keel evolution? Geosci Front 10(5):1765–1787. https://doi.org/10.1016/j.gsf.2019.02.009

19. Farina F, Albert C, Martínez Dopico C, Aguilar Gil C, Moreira H, Hippertt JP, Cutts K, Alkmim FF, Lana C (2016) The Archean-Paleoproterozoic evolution of the Quadrilátero Ferrífero (Brasil): current models and open questions. J S Am Earth Sci 68:4–21. https://doi.org/10.1016/j.jsames.2015.10.015
20. Ladeira EA, Viveiros JFM (1984) Hipótese sobre a estruturação do Quadrilátero Ferrífero com base em dados disponíveis. Boletim da Sociedade Brasileira de Geologia-Núcleo Minas Gerais 4:1–14
21. Rosière CA, Siemes H, Quade H, Brokmeier HG, Jansen EM (2001) Microstructures, textures and deformation mechanisms in hematite. J Struct Geol 23(9):1429–1440. https://doi.org/10.1016/S0191-8141(01)00009-8
22. Zucchetti M, Lobato L, Baltazar O (2000) Volcanic and volcaniclastic features in Archean rocks and their tectonic environments, Rio das Velhas Greenstone Belt, Quadrilátero Ferrífero, MG, Brazil. Braz J Geol 30(3):388–392. https://doi.org/10.25249/0375-7536.2000303388392
23. Brajnikov B (1947) Essai sur la tectonique de la région a l'est de Belo Horizonte, Minas Gerais, Brésil. Bulletin de la Société Géologique de France S5-XVII:321–335. https://doi.org/10.2113/gssgfbull.S5-XVII.4-6.321
24. Hasui Y (1990) Neotectônica e aspectos fundamentais da tectônica ressurgente no Brasil. Brasil. Boletim da Sociedade Brasileira de Geologia, Núcleo de Minas Gerais 11:1–31
25. Saadi A, Rosière CA, Sgarbi GNC (1992) A bacia de Congo Soco, nova bacia terciária no Quadrilátero Ferrífero: controle cárstico e/ou tectônico. In*: Anais do XXXVII Congresso Brasileiro de Geologia* (pp. 600–601). São Paulo: Sociedade Brasileira Geologia
26. Sgarbi GNC, Fantinel LM, Masoti FS (1992) Geologia dos sedimentos lacustres da bacia Terciária de Gandarela, MG. Revista da Escola de Minas 45:118–122
27. Saadi A (1993) Neotectônica e tectônica recente na porção sul do Cráton do São Francisco. In*: Anais do II Simpósio do Cráton do São Francisco. Sociedade Brasileira Geologia, Núcleo Bahia/Sergipe, Salvador* (pp. 230–232). Salvador: Sociedade Brasileira Geologia
28. Sant'Anna LG, Schorscher HD, Riccomini C (1997) Cenozoic tectonics of the Fonseca basin region, eastern Quadrilátero Ferrífero, MG, Brazil. J S Am Earth Sci 10(3–4):275–284. https://doi.org/10.1016/s0895-9811(97)00016-3
29. Agurto-Detzel H, Bianchi M, Assumpção M, Schimmel M, Collaço B, Ciardelli C, Barbosa JR, Calhau J (2016) The tailings dam failure of 5 November 2015 in SE Brazil and its preceding seismic sequence. Geophys Res Lett 43:4929–4936. https://doi.org/10.1002/2016GL069257
30. Centro de Sismologia da Universidade de São Paulo (2019) Seismological report for Monday, 25 November 2019. http://moho.iag.usp.br/eq/latest
31. Guild PW (1957) Geology and mineral resources of the Congonhas district, Minas Gerais, Brazil. USGS Professional Paper 290. https://doi.org/10.3133/pp290
32. Lisboa MA (1898) O manganez no Brazil: contribuição ao estudo das jazidas mineraes brazileiras. Typografia do Jornal do Commercio, Rio de Janeiro
33. Scott HK (1900) The manganese ores of Brazil. J Iron Steel Inst 57:179–208
34. Alkmim F, Marshak S (1998) Transamazonian orogeny in the southern São Francisco craton region, Minas Gerais, Brazil: Evidence for Paleoproterozoic collision and collapse in the Quadrilátero Ferrífero. Precambr Res 90:29–35. https://doi.org/10.1016/s0301-9268(98)00032-1
35. Dorr JVN II (1969) Physiographic, stratigraphic, and structural development of the Quadrilátero Ferrífero, Minas Gerais, Brazil. USGS Professional Paper 641-A. https://doi.org/10.3133/pp641A
36. Endo I (1997) Regimes tectônicos do Arqueano e Proterozóico no interior da placa Sanfranciscana: Quadrilátero Ferrífero e áreas adjacentes. Doctoral thesis, Instituto de Geociências, Universidade de São Paulo. https://www.teses.usp.br/teses/disponiveis/44/44134/tde-12112015-111453/publico/Endo_Doutorado.pdf
37. Hippertt J, Davis B (2000) Dome emplacement and formation of kilometre-scale synclines in a granite–greenstone terrain (Quadrilátero Ferrífero, southeastern Brazil). Precambr Res 102(1–2):99–121. https://doi.org/10.1016/S0301-9268(00)00061-9
38. Endo I, Delgado C, Oliveira M, Zapparoli A, Carlos D, Galbiatti HF, Castro P, Suita MT, Barbosa MS, Lana CE (2019) Mapa geológico do Quadrilátero Ferrífero, escala 1:150.000: revisado e atualizado. Escola de Minas, Universidade Federal de Ouro Preto, Minas Gerais, Brazil
39. Gorceix H (1884) Bacias terciárias d'água doce nos arredores de Ouro Preto, Gandarela e Fonseca: Minas Gerais—Brasil. Anais da Escola de Minas de Ouro Preto 3:9–16
40. Maizatto JR (2001) Análise bioestratigráfica, paleoecológica e sedimentológica das bacias terciárias de Fonseca e Gandarela: Quadrilátero Ferrífero—Minas Gerais, com base nos aspectos palinológicos e sedimentares. Doctoral thesis, Departamento de Geologia, Escola de Minas, Universidade Federal de Ouro Preto. http://www.repositorio.ufop.br/handle/123456789/2208
41. de Lima MR, Salard-Cheboldaeff M (1981) Palynologie des bassins de Gandarela et Fonseca (eocene de l'etat de Minas Gerais, Brésil). Boletim IG 12:33–53. https://doi.org/10.11606/issn.2316-8978.v12i0p33-53
42. Harder EC, Chamberlin RT (1915) The geology of central Minas Geraes, Brazil. J Geol 23(5):385–424. https://doi.org/10.1086/622256
43. Maxwell CH (1972) Geology and ore deposits of the Alegria District, Minas Gerais, Brazil. USGS Professional Paper 341-J. https://doi.org/10.3133/pp341J
44. Hu Z, Gao S (2008) Upper crustal abundances of trace elements: a revision and update. Chem Geol 253(3–4):205–221. https://doi.org/10.1016/j.chemgeo.2008.05.010
45. Wedepohl HK (1995) The composition of the continental crust. Geochim Cosmochim Acta 59(7):1217–1232. https://doi.org/10.1016/0016-7037(95)00038-2
46. Richter D (1966) On the new red sandstone Neptunian dykes of the Tor Bay area (Devonshire). Proc Geol Assoc 77(2):173–186. https://doi.org/10.1016/S0016-7878(66)80068-8
47. Bokanda EE, Ekomane E, Eyong JT, Njilah IK, Ashukem EN, Bisong RN, Bisse SB (2018) Genesis of clastic dykes and soft-sediment deformation structures in the Mamfe Basin, South-West Region, Cameroon: field geology approach. J Geol Res 2018:1–8. https://doi.org/10.1155/2018/3749725
48. Jonk R, Hurst A, Duranti D, Parnell J, Mazzini A, Fallick AE (2005) Origin and timing of sand injection, petroleum migration, and diagenesis in Tertiary reservoirs, south Viking Graben. North Sea AAPG Bull 89(3):329–357. https://doi.org/10.1306/10260404020
49. Montenat C, Barrier P, Ott d'Estevou P, Hibsch C (2007) Seismites: an attempt at critical analysis and classification. Sed Geol 196(1–4):5–30. https://doi.org/10.1016/j.sedgeo.2006.08.004
50. Engelder JT (1974) Microscopic wear grooves on slickensides: Indicators of paleoseismicity. J Geophys Res 79(29):4387–4392. https://doi.org/10.1029/jb079i029p04387
51. Piassa L (2018) A Falha do Engenho revisitada: sul do Quadrilátero Ferrífero, Minas Gerais. M.Sc. dissertation, Departamento de Geologia, Escola de Minas, Universidade Federal de Ouro Preto.
52. Cabral AR, Koglin N (2014) Hydrothermal overprint on Cenozoic sediments in the Quadrilátero Ferrífero of Minas Gerais: Implications for precious metals in cratonic terrains. Terra Nova 26(2):11–119. https://doi.org/10.1111/ter.12076
53. Cabral AR, DeFerreira TH, Dias GMC, Silva FG, Soares BDR, Rios FJ (2020) The use of mercury vs. cerium in recognising seismically

induced fluid overprints on weathered profiles. Results Geochem. https://doi.org/10.1016/j.ringeo.2020.100006
54. Cabral AR, Rios FJ, Amorim LED, Laufek F, Martins Graça L (2020) Hydrothermal cerium oxide in manganese-oxide-cemented breccia, Quadrilátero Ferrífero of Minas Gerais, Brazil. N Jb Miner Abh 196(12):231–242. https://doi.org/10.1127/njma/2020/0184
55. Sibson RH, Moore JM, Rankin AH (1975) Seismic pumping—a hydrothermal fluid transport mechanism. J Geol Soc. https://doi.org/10.1144/gsjgs.131.6.0653
56. Crespo A, Lunar R, Oyarzuc R, Doblas M (1995) Unusual case of hot springs-related Co-rich Mn mineralization in central Spain; the Pliocene Calatrava deposits. Econ Geol 90(2):433–437. https://doi.org/10.2113/gsecongeo.90.2.433
57. Guiyin Y, Shanghua Z, Mingkai Z, Jianping D, Deyu L (1992) A new magnesic mineral of the chalcophanite group. Acta Mineral Sinica 12:69–77 (**in Chinese with English abstract**)
58. Hewett DF (1964) Veins of hypogene manganese oxide minerals in the southwestern United States. Econ Geol 59(8):1429–1472. https://doi.org/10.2113/gsecongeo.59.8.1429
59. Miura H, Hariya Y (1997) Recent manganese oxide deposits in Hokkaido, Japan. Geol Soc Spec Pub 119(119):281–299. https://doi.org/10.1144/GSL.SP.1997.119.01.18
60. Moorby SA, Cronan DS, Glasby GP (1984) Geochemistry of hydrothermal Mn-oxide deposits from the S.W. Pacific island arc. Geochim Cosmochim Acta 48(3):433–441. https://doi.org/10.1016/0016-7037(84)90272-2
61. Roy S (1968) Mineralogy of the different genetic types of manganese deposits. Econ Geol 63(7):760–786. https://doi.org/10.2113/gsecongeo.63.7.760
62. Chermak JA, Rimstidt JD (1990) The hydrothermal transformation rate of kaolinite to muscovite/illite. Geochim Cosmochim Acta 54(11):2979–2990. https://doi.org/10.1016/0016-7037(90)90115-2
63. Horton DG (1985) Mixed-layer illite/smectite as a paleotemperature indicator in the Amethyst vein system, Creede district, Colorado, USA. Contrib Miner Pet 91(2):171–179. https://doi.org/10.1007/BF00377764
64. McDowell SD, Elders WA (1980) Authigenic layer silicate minerals in borehole Elmore 1, Salton Sea Geothermal Field, California, USA. Contrib Miner Petrol 74:293–310. https://doi.org/10.1007/BF00371699
65. Yangfen J, Zonghua W, Chunsheng S, Jiazhen W, Hongren Z (1989) Earthquake prediction through the observation and measurement of mercury content variation in water. J Geochem Explor 33(1–3):195–202. https://doi.org/10.1016/0375-6742(89)90029-0
66. Zhang L, Liu Y, Guo L, Yang D, Fang Z, Chen T, Ren H, Yu B (2014) Isotope geochemistry of mercury and its relation to earthquake in the Wenchuan earthquake fault scientific drilling project hole-1 (WFSD-1). Tectonophysics 619–620:9–85. https://doi.org/10.1016/j.tecto.2013.08.025
67. Christensen OD, Capuano RA, Moore JN (1983) Trace-element distribution in an active hydrothermal system, Roosevelt hot springs thermal area, Utah. J Volcanol Geoth Res 16(1–2):99–129. https://doi.org/10.1016/0377-0273(83)90086-0
68. Pohl WL (2011) Economic geology principles and practice. Wiley-Blackwell, Oxford
69. Rodríguez-Díaz AA, Canet C, Villanueva-Estrada RE, Chacón E, Gervilla F, Velasco-Tapia F, Cruz-Gámez EM, González-Partida E, Casas-García R, Linares-López C, Pérez-Zárate D (2019) Recent Mn-Ag deposits in coastal hydrothermal springs in the Baja California Peninsula, Mexico. Miner Depos 54(6):849–866. https://doi.org/10.1007/s00126-018-0846-9
70. Hussak E (1897) Das Zinnober-Vorkommen von Tripuhy in Minas Geraes, Brasilien. Zeit prak Geol 5:65–67
71. Cabral AR, Corrêa Neto AV (2006) Mercury-bearing manganiferous veinlets in compact haematite ore: the preliminary data from Fábrica deposit, Quadrilátero Ferrífero, Minas Gerais, Brazil. Appl Earth Sci 115:1–7. https://doi.org/10.1179/174327506X111264
72. Santos MC, Varajão AFDC, Yvon J (2004) Genesis of clayey bodies in Quadrilátero Ferrífero, Minas Gerais, Brazil. Catena 55(3):277–291. https://doi.org/10.1016/S0341-8162(03)00106-1
73. Shuster DL, Farley KA, Vasconcelos PM, Balco G, Waltenberg K, Monteiro HS, Stone JO (2012) Cosmogenic ^{3}He in hematite and goethite from Brazilian "canga" duricrust demonstrates the extreme stability of these surfaces. Earth Planet Sci Lett 329–330:41–50. https://doi.org/10.1016/j.epsl.2012.02.017
74. Spier CA, Vasconcelos PM, Oliviera SMB (2006) ^{40}Ar/^{39}Ar geochronological constraints on the evolution of lateritic iron deposits in the Quadrilátero Ferrífero, Minas Gerais, Brazil. Chem Geol 234(1–2):79–104. https://doi.org/10.1016/j.chemgeo.2006.04.006
75. Varajão CAC, Salgado AAR, Varajão AFDC, Braucher R, Colin F, Nalini HÁ Jr (2009) Estudo da evolução da paisagem do Quadrilátero Ferrífero (Minas Gerais, Brasil). Rev Bras Cienc Solo 33(6):1409–1425
76. Lavarini C, Magalhães Júnior AP, de Oliveira FS, de Carvalho A (2016) Neotectonics, river capture and landscape evolution in the highlands of SE Brazil. Mercator 15(4):95–119. https://doi.org/10.4215/RM2016.1504.0007
77. Assumpção M, Ferreira J, Barros L, Bezerra H, França GS, Barbosa JR, Menezes E, Ribotta LC, Pirchiner M, Nascimento A, Dourado J (2012) Intraplate seismicity in Brazil. In: Talwani P (ed) Intraplate earthquakes. Cambridge University Press, Cambridge, pp 50–71. https://doi.org/10.1017/CBO9781139628921.004
78. Assumpção M, Suárez G (1988) Source mechanisms of moderate-size earthquakes and stress orientation in mid-plate South America. Geophys J 92(2):253–267. https://doi.org/10.1111/j.1365-246X.1988.tb01138.x
79. CODEMIG (2005) Geologia do Quadrilátero Ferrífero – integração e correção cartográfica em SIG. Companhia de Desenvolvimento Econômico de Minas Gerais, Belo Horizonte, Brazil